International Communications in Heat and Mass Transfer 38 (2011) 1044–1049

Contents lists available at ScienceDirect

International Communications in Heat and Mass Transfer

journal homepage: www.elsevier.com/locate/ichmt

Experimental and numerical study on air cores for cylindrical tank draining ☆

Il Seouk Park, Chang Hyun Sohn *

School of Mechanical Engineering, Kyungpook National University, 1370, Sangyeok-dong, Buk-gu, Daegu, 702-701, South Korea

ARTICLE INFO

Available online 20 May 2011

Keywords:
Air core
Swirl velocity
Vorticity
Draining

ABSTRACT

An air core is generated during draining after rotating cylindrical tanks filled with liquid. Air cores have a complex flow structure including rotational motion and a change in the free surface shape. In addition, the generation and extinction of air cores are dependent on the initial rotating speed, the dimensions of the tank, and the liquid materials. This phenomenon is usually detected in various applications for different fields such as the flow in the tundish discharging process of the smelting process, the liquid fuel system of rockets, from the suction of pumps, and so on. In this study, the flow structures including the drain time, the change in the free surface shape, velocity field, and vorticity distributions are numerically and experimentally investigated. Both the numerically and experimentally results were in good agreement with each other with respect to the drain time.

1. Introduction

An air core can generate when liquid is drained through a hole centered on the bottom of a cylindrical tank after the free surface level reaches a critical height. The presence of initial rotation can augment the air core formation.

The air core has a spiral shape like a tornado piercing through the upper surface of the liquid to the bottom of the tank. The effective sectional area for the drain outlet becomes narrow because the area parting with the gas phase increases. Thus, the draining flow rate is significantly affected by the existence of the air core[1]. Tundish discharging process between the smelting process and continuous casting process (see Fig. 1 (a)) accompanies a very similar physical phenomenon to this. In that process, the air core non-uniformly entrains and discharges slag and additives floating on a free surface to a slab. Ultimately, it makes the slab inferior and the cost higher. In liquid rocket fuel systems, the air core generated by external disturbances diminishes the trust, entrains air bubbles, and makes the combustion unstable[2,3]. In a sump pump station, a swirling flow can initiate by the operation of the pump (see Fig. 1 (b)), and air core can form. The air enters the pump. The entrained air causes trouble such as cavitation on the pump blades, degrading the pump's efficiency, vibrations, noise, and so on[4,5]. To prevent the generation of an air core, Gowda et al. [6] used a dish-type suppressor and Sohn et al. [7] studied the effect of the eccentric drain port position. From previous studies, Sohn et al. [8] captured the flow structure in a cylindrical tank using PIV (Particle Image Velocimetry) for the vane-type vortex suppressor. To prevent the generation of an air core, Sohn et al. [9] experimentally studied the effect of corner radius on a square cylinder.

In the present study, the draining with air core phenomenon was numerically investigated. The flow structures in a circular tank accompanying the air core were examined in association with the generation of the air core. The non-swirling case (no air core) was also simulated to check the drain time lag caused by the air core. The drain process was visualized by experimental methods and compared with the computational results with respect to not only the free surface shapes in a tank but also the drain time.

2. Numerical analysis

To describe the swirling and draining flow in a tank, the axisymmetric equation set for the mass and momentum conservation was selected. Although the actual draining process accompanies a spiral motion on the free surface, the flow field is assumed to be an axisymmetric swirling flow to avoid the complexity related to solving a three-dimensional process. Axisymmetric assumption was satisfactory for the capture of the air core phenomenon demonstrated by the numerical analysis in this study.

To find the swirl velocity component in a two-dimensional grid system, the following conservation equation for the tangential momentum was applied in addition to the basic axisymmetric governing equation set.

$$\frac{\partial}{\partial z}(r\rho u_z u_\theta) + \frac{\partial}{\partial r}(r\rho u_r u_\theta) = \frac{\partial}{\partial z}\left(r\mu\frac{\partial u_\theta}{\partial z}\right) + \frac{1}{r}\frac{\partial}{\partial r}\left(r^3\mu\frac{\partial}{\partial r}\left(\frac{u_\theta}{r}\right)\right) - \rho u_r u_\theta \quad (1)$$

Here, z is the axial component of the coordinate system, r the radial coordinate component, u_r the radial velocity component, u_θ the tangential velocity component, ρ the density, and μ the dynamic viscosity. This is very useful and practical in terms of the computational cost

☆ Communicated by W. J. Minkowycz.

* Corresponding author.
E-mail address: chsohn@knu.ac.kr (C.H. Sohn).

0735-1933/$ – see front matter © 2011 Elsevier Ltd. All rights reserved.
doi:10.1016/j.icheatmasstransfer.2011.05.002

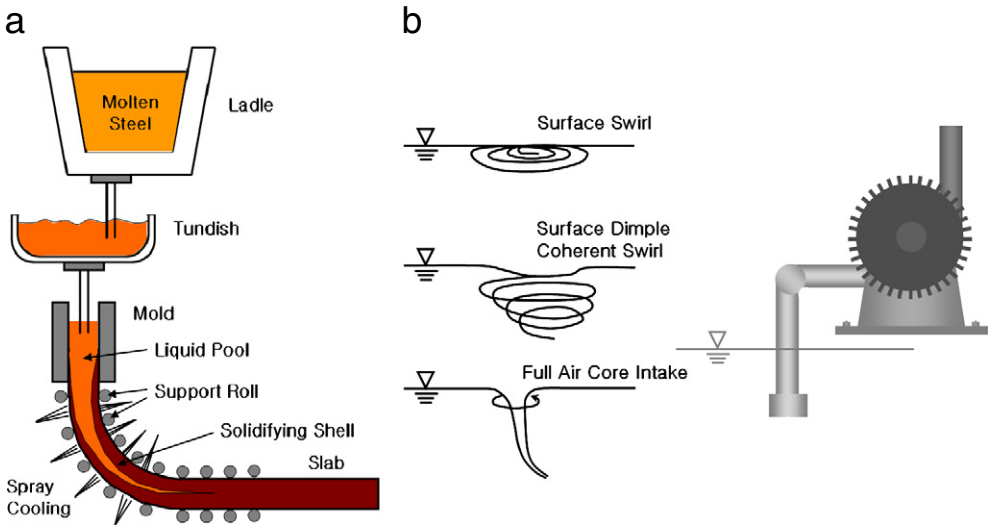

Fig. 1. (a) Tundish in the continuous casting process, (b) air core phenomenon by a suction pump.

because the high level flow information including all three velocity components can be obtained just on a two-dimensional mesh system.

The liquid in a tank initially moves like a rigid body with the side wall rotating with an angular velocity of 120 rpm. The cylinder wall rotation stops for 3 s before starting the draining of liquid. This stoppage period is the time for manipulating the drain valve in this experiment. The present numerical simulation took into account these all flow sections from the experimental setup with the flow assumed to be in the laminar form.

To capture the liquid-air interface, the VOF(Volume Of Fluid) scheme [10] was adopted. For more precise tracking of the free surface, PLIC (Piecewise Linear Interface Computation) scheme was applied which was suggested by Youngs [11] and known as the Geo-Reconstruct in the commercial CFD code Fluent 6.3 [12]. All governing equations including VOF were solved by Fluent 6.3. Implicit time marching was applied for the flow variables. But for interface capturing, the explicit time marching was applied to shorten the time-consuming free surface capturing process in the PLIC. The surface tension coefficient was 0.0712 *N/m*. All the cases in this paper were solved on a two dimensional mesh of 17,600 cells as shown in Fig. 2. The time increment was set as 1×10^{-3}~1×10^{-4} s.

3. Experiment

Fig. 3 shows the apparatus for the liquid draining experiment. The cylindrical tank has a height of 450 mm, an inner diameter of 90 mm, a drain nozzle length of 15 mm, and a drain nozzle inner diameter of 6 mm. The control system for tank rotating speed was located beside the support frame under the test section. To capture the instantaneous flow image, a diode laser (820 mW) and Redlake MotionPro X53 high speed CCD camera were used as shown in Fig. 3. First, the tank was filled up with liquid water to a level of 350 mm from the bottom of the tank. For the non-swirling case, the liquid started to drain right after the free surface became stable. For the swirling case, the tank was rotated with an angular velocity of 120 rpm. At lower values of RPM, the critical height which the air core forms depends on the magnitude of the rotation given. However, for 90 rpm and above, the critical height does not vary considerably [6]. The tank rotation was maintained for about 10 s until the flow reached a steady state.

For the liquid level over time, the positions of the contact point of the liquid on the tank side wall were measured. The time was recorded when measuring the level as it passed through every 20 mm increment. The time the tank took to be drained completely was also recorded.

The drain time can theoretically be estimated with the following equation.

$$t = \frac{\sqrt{h_0}-\sqrt{h}}{\alpha\sqrt{g/2}}\left(\frac{d_c}{d_n}\right)^2 \tag{2}$$

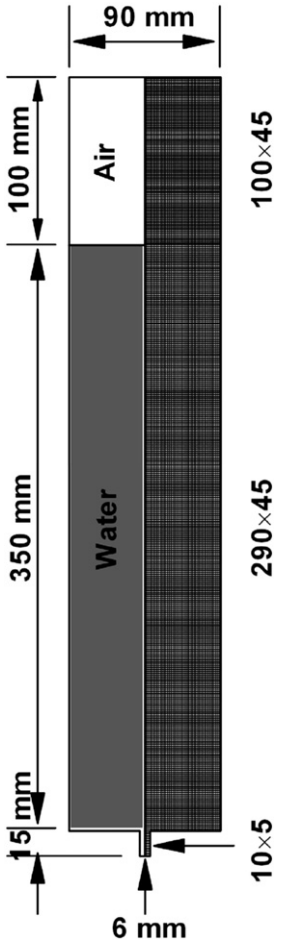

Fig. 2. Schematics and grid system of the calculation domain.

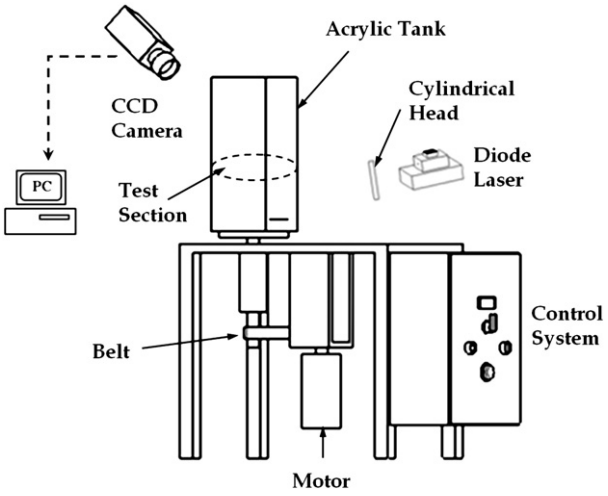

Fig. 3. Experimental apparatus.

Eq. (2) is derived from the mass conservation in a tank[13].t is the drain time, h_0 the initial liquid level, h the liquid level at specific time, g the gravitational acceleration, d_c the cylinder tank diameter, d_n the drain nozzle diameter, and α the empirical coefficient. The above equation is derived under the assumptions of no-viscous friction and the no-swirling flow. Therefore, to compensate for those, the empirical coefficient α was applied.

4. Results and discussions

4.1. Comparison of the draining time

Table 1 shows the draining time for the liquid level on the side wall obtained experimentally, numerically, and theoretically in both of the initial rotating and non-rotating cases. All experimental results were obtained from more than 20 independently repeated experiments to confirm reproducibility. The standard deviation for the draining time was about 0.27 s for the initial non-swirling case, and 0.83 s for initial swirling case. The empirical coefficient in the theoretical results (see. Eq. (2)) was 0.86 for the non-swirling case and 0.71 for the swirling case. These values were obtained from minimizing the root mean square for the difference between the experimental results and the theoretical results.

Table 1
The drain time of the non-swirling case and the swirling case.

Free surface level [mm]	Non-swirl case			Swirl case		
	Exp. [s]	Theo. [s]	Num [s]	Exp. [s]	Theo. [s]	Num [s]
350	0.0	0.0	0.0	0.0	0.0	0.0
330	2.21	2.00	1.98	1.96	2.42	2.30
310	4.28	4.07	5.14	4.16	4.91	4.50
290	6.57	6.20	7.81	6.84	7.49	6.85
270	8.89	8.41	9.96	10.74	10.16	10.28
250	11.44	10.70	12.52	14.56	12.93	14.60
230	14.12	13.08	16.54	17.98	15.81	18.76
210	16.59	15.57	19.04	20.85	18.82	22.94
190	19.29	18.18	22.26	23.70	25.30	31.32
170	22.11	20.94	24.17	26.70	25.30	31.32
150	25.13	23.86	26.29	29.86	28.83	35.65
130	28.22	26.98	30.65	33.14	32.60	39.65
110	31.63	30.35	35.03	36.71	36.68	43.87
90	35.26	34.05	39.98	40.52	41.15	48.27
70	37.56	38.19	45.87	45.19	46.14	53.42
50	43.68	42.97	50.21	51.57	51.93	59.07
30	48.82	48.86	55.38	60.21	59.04	66.01
10	55.12	57.41	59.86	72.59	69.37	75.38
0	58.16	69.08	63.18	80.26	83.48	82.32

Fig. 4 shows the draining time for each case. In both the swirling and non-swirling cases, the numerical results show a rather slower draining time compared to the experimental results. But the draining completion times were similar to each other. For the non-swirling case, the difference in the draining completion time between the numerical simulation and experimental was about 5 s. For the swirling case, the value was about 2 s. The swirling case required about a 30% longer time to complete the draining (about 20 s) compared to the non-swirling case because of the reduction effect of the exit area.

4.2. Generation of air core

Fig. 5 shows the process for the generation of the air core from the numerical simulation. The dip shape of the free surface at the early stage was due to the rigid body behavior of the liquid in a tank before the draining starts. The shape of dip at the early stage first flattened from the stopping rotation. But starting from a point of 3 s, the sinking phenomenon was detected nearby in the center area. At 8 s, the air core was completely generated. The air core penetrated from the top face of the free surface to the drain port. The generated air core was continuously maintained and did not vanish until the draining finished. The effective exit section was reduced because the air occupied the center portion of the drain nozzle. Thus, the flow rate for draining decreased and the draining completion time increased.

Fig. 6 shows experimental results of the generation of an air core. The overall shapes of the free surfaces and the liquid level show a very similar pattern to the numerical results. Air core penetration occurred at 6 s for the experimental model while at 8 s for the numerical simulation.

4.3. Swirl velocity in a tank

Fig. 7 shows the swirl velocity distribution in a circular tank from the draining start. The swirl velocity at the early stage was caused by the side-wall rotation before the draining. Thus, the magnitude was comparatively high near the side wall. As time goes on, the maximum swirl velocity zone moved to the inner area because of the growth of the boundary layer on the side wall and balance of angular momentum. Such a boundary layer also formed on the bottom wall region, which is called the Ekman spiral layer. Based on the Ekman spiral suction flow, the fluid flowing to the tank center from the side wall in the top area of the liquid has a larger swirl velocity due to the angular

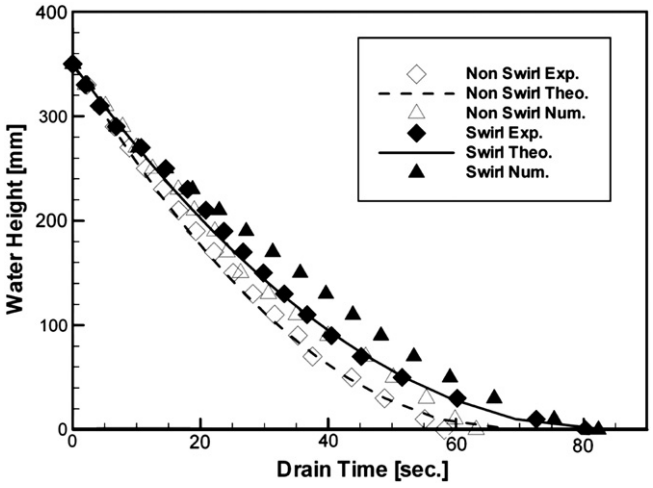

Fig. 4. Drain time of the non-swirling case and swirling case by theoretical, experimental and numerical methods.

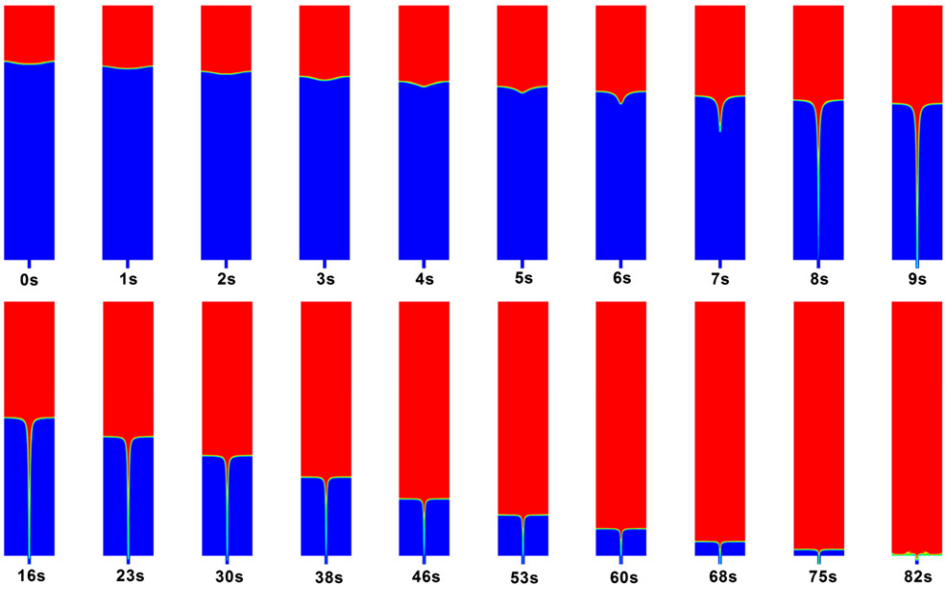

Fig. 5. Generation and progression of the air core from the numerical simulation (0–82 s).

momentum conservation and flows down to the bottom of the tank. Besides this due to the draining, the liquid layer with a high angular momentum on the bottom center area entrains to the drain port. As a result of these, a very high swirl velocity is measured near the drain port. This high swirl velocity region moves upward rapidly along the free surface in accompanying the generation of the air core. After 60 s from the start of draining, the swirl velocity starts to gradually become extinct.

4.4. Vorticity in a tank

Fig. 8 shows the vorticity distribution in a tank from the start of draining. In the early stage, small vorticity cells were detected near the side wall because of the no-slip effect. These vorticity cells are well known as the Taylor vortex having a circumferential axis. The vorticity in a tank can be represented by the following Eq. (3) in an axisymmetric circumstance.

$$\vec{\zeta} = \nabla \times \vec{v} = -\frac{\partial v_\theta}{\partial z}\hat{r} + \left(\frac{\partial v_r}{\partial z} - \frac{\partial v_z}{\partial r}\right)\hat{\theta} + \frac{1}{r}\frac{\partial (r v_\theta)}{\partial r}\hat{z} \tag{3}$$

The Taylor vortex beside the side wall in the circumferential direction is clearly related with the axial velocity gradient in the radial direction and the radial velocity gradient in the axial direction as shown in the second term of Eq. (3). The distributions of the radial and axial velocities on the longitudinal section are crossly connected with the draining process. In fact, Sohn [7] considered the position of the drain port as the vital factor in the generation of air cores. Since the eccentric drain port problem needs a three dimensional simulation, it was excluded in the present study but will be considered in a near future study. Besides the side Taylor vortex, the significant magnitude

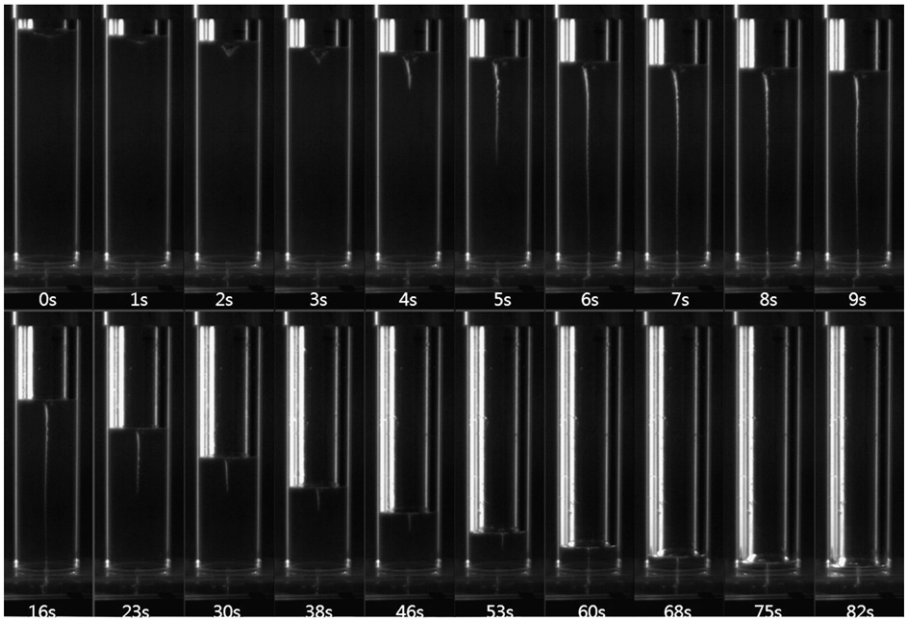

Fig. 6. Generation and progression of the air core with the experiment apparatus (0–82 s).

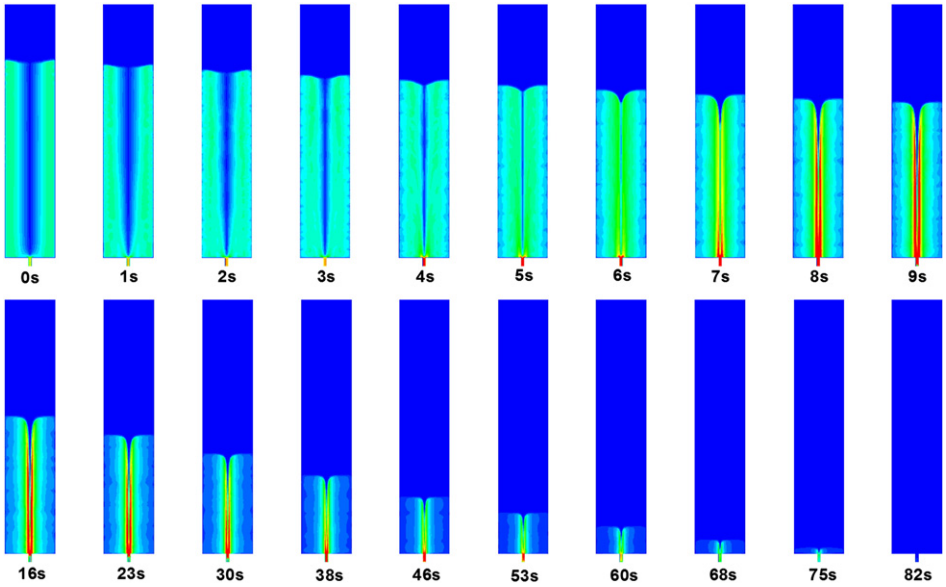

Fig. 7. Progression of the swirl velocity distribution. (0–82 s).

of the vorticity was measured near the drain port. This is related to the last term of Eq. (3) and has a rotating axis in the axial direction. Due to the draining, the swirl velocity near the drain port was significantly increased as described earlier in Fig. 7, and thus, the angular velocity gradient in the radial direction is increased nearby in the bottom center area. This vortex in the axial direction gradually prevailed in the overall domain interacting with a secondary vortex (Taylor vortex) nearby the side wall, and diminished the secondary vortex. The suction flow was initiated in the center area because of the Ekman suction on the bottom area to conserve the angular momentum and became stronger due to the draining effect. As a result of these processes, the air core was generated in the center area.

5. Conclusions

In this study, the simulation of the air core phenomenon was investigated before suggesting more active or effective air core suppressing devices. The simulation results were compared with the experimental ones and were in good agreement in terms of the draining time and the free surface shape progression during the process of developing an air core. It was revealed that the generation of air cores are related to both the Ekman suction and the draining effect. During the progression of an air core, the vortices in the various directions including the Taylor vortex and the Ekman swirl, and their interacting processes were clearly represented on the meridian section. The present results will be useful in making the right decision among the various choices for protecting against the generation of air cores in accordance with the corresponding circumstances.

Acknowledgements

This research was supported by Basic Science Research Program through the National Research Foundation of Korea(NRF) funded by the Ministry of Education, Science and Technology(the Grant 2010–0025260).

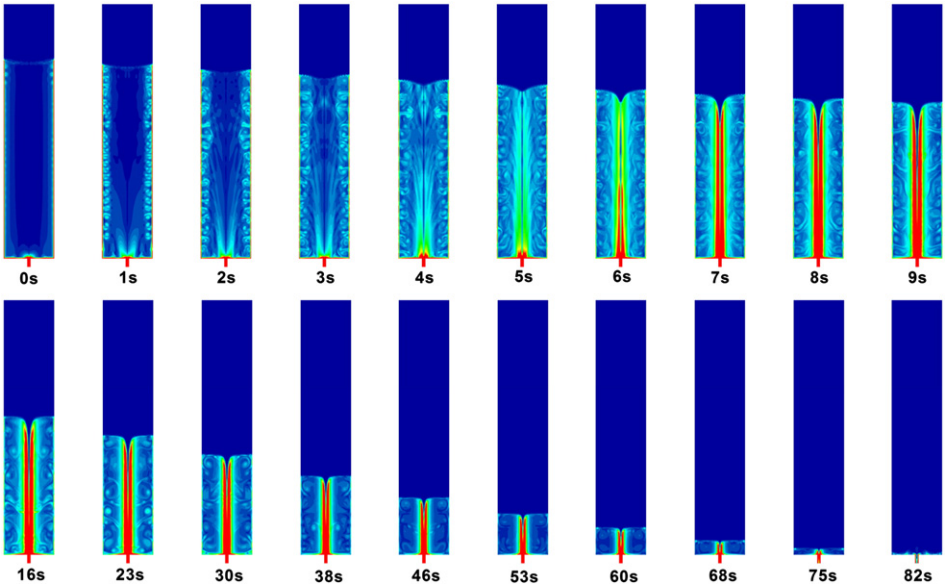

Fig. 8. Progression of the vorticity distribution (0–82 s).

References

[1] Q.N. Zhou, W.P. Graebel, Axisymmetric draining of cylindrical tank with a free surface, J. Fluid Mech. 221 (1990) 511–532.
[2] H.N. Abramson, W.H. Chu, L.R. Garza, G.E. Ransleben, Some studies of liquid rotation and vortexing in rocket propellant tanks, NASA D-1212 (1962) 1–35.
[3] G.F. Pasley, Propellant vortexing in a spinning spacecraft, Journal of Spacecraft and Rockets 18 (5) (1981) 418–426.
[4] D.I. Bauer, T. Nakato, Subsurface vortex suppression in water intakes with multiple-pump sumps, iihr technical report no. 389, Iowa Institute of Hydraulic Research, 1997 1–81.
[5] J.W. Choi, Y.D. Choi, W.S. Lim, Y.H. Lee, Numerical analysis on the flow uniformity in a pump sump model with multi pump intake, Journal of Fluid Machinery 12 (4) (2009) 14–22.
[6] B.H.L. Gowda, P.J. Joshy, S. Swarnamani, Device to suppress vortexing during draining from cylindrical tanks, Journal of Spacecraft and Rockets (AIAA) 33 (1996) 598–600.
[7] C.H. Sohn, B.H.L. Gowda, M.G. Ju, Eccentric drain port to prevent vortexing during draining from cylindrical tanks, Journal of Spacecraft and Rockets 45 (3) (2008) 638–640.
[8] C.H. Sohn, M.G. Ju, B.H.L. Gowda, Draining from cylindrical tanks with vane-type suppressors — a PIV study, J. Visualization 12 (4) (2009) 347–360.
[9] C.H. Sohn, M.G. Ju, B.H.L. Gowda, PIV study of vortexing during draining from square tanks, Journal of Mechanical Science and Technology 24 (2010) 951–960.
[10] C.W. Hirt, B.D. Nichols, Volume of Fluid (VOF) method for the dynamics of free boundaries, Journal of Computational Physics 39 (1981) 201–225.
[11] D.L. Youngs, Time-Dependent Multi-Material Flow with Large Fluid Distortion, Academic Press, Numerical Methods for Fluid Dynamics, 1982 273–285.
[12] Fluent 6.3 Users Guide, Fluent Inc, 2006.
[13] Y.A. Cengel, J.M. Cimbala, Fluid mechanics Fundamentals and Applications, McGraw-Hill Higher Education (2008) 166–189.